The RXTE All Sky Monitor: First Year of Performance

Ronald A. Remillard[1] and Alan M. Levine[1]

[1] Center for Space Research, Massachusetts Institute of Technology, Cambridge MA 02139 USA
E-mail: rr@space.mit.edu

Abstract

The RXTE All Sky Monitor provides a public database that includes more than one year of X-ray monitoring observations (2-12 keV) of X-ray binaries and a few active galactic nuclei. The instrument operates with a 40% duty cycle, and the exposures yield roughly 5 celestial scans per day. There have been 109 source detections, including 16 X-ray transients, the majority of which are recurrent cases. The two sources of relativistic radio jets have exhibited particularly complex light curves and new types of emission states. Progress has been achieved in understanding the outburst mechanism via the reported detection of an optical precursor to the April 1996 X-ray outburst in GRO J1655-40. The ASM has also detected state changes in both Cyg X-1 and Cyg X-3, leading to new constraints on the accretion disk geometry associated with the "soft/high" state. X-ray variations are seen in extragalactic nuclei, such as NGC4151 and Mkn501, providing new opportunities for multifrequency timing or spectral studies. The ASM archive empowers observers with the opportunity for state-dependent observing programs with RXTE and other instruments. The ASM also provides a long-term context for source behavior, and this knowledge may be crucial in shaping the interpretation of brief observations with other telescopes.

Key words: surveys — X-rays: general — X-rays: stars

1. Introduction

The All Sky Monitor (ASM) on the *Rossi X-ray Timing Explorer* (RXTE) has been regularly observing bright celestial X-ray sources since 1996 February 22. Detector problems had been encountered during the first days of operation (1996 January 5-12), but the instrument has remained stable under an operation plan restricted to low-background regions of the RXTE orbit (580 km altitude). In addition there is an on-board monitor system that switches off high voltage in the event of moderately high rates in any of several different measures of the detector background. The ASM currently operates with 20 of the original 24 detector anodes, and the typical observation duty cycle is 40%, with the remainder of the time lost to the high-background regions of the orbit, spacecraft slews, and instrument rotation or rewinds. The net yield from the ASM exposures is about 5 celestial scans per day, excluding regions near the Sun. All of the ASM calibrations, data archiving, the derivation of source intensities, and efforts to find new sources are carried out with integrated efforts of the PI team at M.I.T. and the RXTE Science Operations Center at Goddard Space Flight Center.

The ASM instrument consists of three scanning shadow cameras (SSC) attached to a rotating pedestal. Each camera contains a position-sensitive proportional counter, mounted below a wide-field collimator that restricts the field of view (FOV) to 6^o x 90^o FWHM and 12^o x 110^o FWZI. One camera (SSC3) points in the same direction as the ASM rotation axis. The other two SSCs are pointed perpendicular to SSC3. The latter cameras face the same direction but the long axes of their collimators are tilted by $+12^o$ and -12^o, respectively, relative to the ASM rotation axis. The ASM can be rotated so that the co-pointing SSCs are aligned with the larger instruments of RXTE (i.e. the PCA and HEXTE). The top of each collimator is covered with an aluminum plate perforated by 6 parallel (and different) series of narrow, rectangular slits that function as a coded mask by casting a two-dimensional shadow pattern for each X-ray source in the collimator's field of view. Further information on this instrument is given by Levine et al. (1996).

The ASM raw data includes 3 types of data products that are tabulated and formatted for telemetry by the two ASM event analyzers in the RXTE Experiment Data System. In the current observing mode, position histograms are accumulated for 90 s "dwells" in which the cameras' FOVs are fixed on the sky. Each dwell is followed by a 6^o instrument rotation to observe the adjacent patch of sky. The rotation plans for ASM dwell sequences are chosen to avoid having any portions of the Earth in the FOVs of SSCs 1 and 2. The position histograms are accumulated in three energy chan-

nels: 1.5-3.0, 3-5, and 5-12 keV. The second data product consists of various measurements from each camera binned in time. These data are useful in studying bright X-ray pulsars, bursters, gamma ray bursts, and several other categories of rapid variability. The "good events" from each camera are recorded for each energy channel in 0.125 s bins, while 6 different types of background measures are recorded in 1 s bins. Finally, 64-channel X-ray spectra from each camera are output every 64 s. These data provide a means of monitoring the detector gain, since we may integrate the spectra over long time scales to observe the 5.9 keV emission line from the weak ^{55}Fe calibration sources mounted in each collimator. In addition, ASM spectra may be useful in investigations of spectral changes in very bright X-ray sources.

The ASM data archive is a public resource available for both planning purposes and scientific analysis. The "realtime" and archived source histories are available in FITS format from the RXTE guest observer facility: http://heasarc.gsfc.nasa.gov/docs/xte/xte_1st.html. The ASM archive is also available in ASCII table format from the ASM web site at M.I.T.: http://space.mit.edu/XTE/XTE.html.

2. ASM Performance and Systematic Issues

Since this forum addresses many instrumental topics related to all-sky monitors, we briefly review performance and calibration issues encountered with the RXTE ASM. The static model for the position of the cameras and the ASM rotation axis yields a net uncertainty (rms) of about 45", as determined from observations of Sco X-1. We minimize the effects of this uncertainty by allowing a camera position to float during data analysis, using chi square to obtain the best fit for detected X-ray sources that lie in a camera's FOV. We estimate that the ASM will obtain positions for new X-ray sources with uncertainties of 2' to 12' for sources in range of 1 Crab to 30 mCrab, respectively.

The core of the ASM analysis task is to deconvolve the position histograms into the X-ray shadow patterns for individual X-ray sources. Our geometric model for the mask, collimator, and anode alignments was significantly revised in 1997 Jan, leading to a complete re-analysis of the ASM database. The primary feature of this revision was the introduction of time-dependent calibrations of the physical to "electronic" position relationships that governs the locations of mask shadows in the position histograms. Observations of Sco X-1 clearly demonstrated variable degrees of evolution of each anode, appearing as secular shifts in the shadow boundaries in the position histograms. The ASM position calibrations are now periodically revised, and the analysis system computes models for individual mask shadows by interpolating or extrapolating from these calibrations for each detector anode.

The observations of the Crab Nebula provide a means of gauging the magnitude of systematic noise in the ASM light curves. The observed variance of the derived intensities is slightly larger than the estimated statistical variance, implying a systematic uncertainty of 1.9% of the mean flux. For faint X-ray sources, systematic effects can be quantified by investigating the light curves for "blank field" positions and quiescent X-ray novae. By binning the ASM source intensities on very long time scales (e.g. 1 year), there is a +1 mCrab bias in the distribution of mean values. The net effect of systematic and statistical limitations allows the ASM to reach 5 mCrab at 3 σ significance in a typical daily exposure (2-12 keV). All of these uncertainty estimates pertain to celestial positions well separated from the Galactic center, where source confusion increases systematic problems.

The observations of the "polar" AM Her serves to illustrate the accuracy achieved in the ASM instrument model. There are no significant detections of this source with the ASM at 1-day time scales. The global average for this source (adjusting for the bias mentioned above) is only 2.3 mCrab. However, the analysis of the individual measurements clearly reveals a periodic signal at 3.0943 ± 0.0001 hr, which is consistent with the known binary period (Ritter and Kolb 1995).

3. Highlights of ASM Results

Many of the results of ASM science investigations fall under four categories which are outlined below. Under each topic, we discuss representative cases that illustrate the value of monitoring observations and the effectiveness of the ASM alarm system in attracting observations at other wavelengths.

3.1. Light Curves of X-ray Transients

There has been a remarkable diversity of active X-ray transients during 1996 and 1997. The prolonged outbursts from the 2 sources of relativistic radio jets, GRS1915+105 (X-ray Nova Aql 1992) and GROJ1655-40 (X-ray Nova Sco 1994), further distinguished these sources from the typical soft X-ray transients. The ASM light curve for GRS1915+105 displays the unique behavior of this source, as it wanders through four emission states that appear to be new variants of the "very high" X-ray state of black hole binaries (Morgan, Remillard, and Greiner 1997; MGR97). Many observatories, including the revitalized Greenbank Interferometer (http://info.gb.nrao.edu/gbint/GBINT.html), are now monitoring the behavior of GRS1915+105. Many groups have begun the investigation of the complex interrelations between radio emission, IR variations, soft X-ray instability, and hard X-ray flares in GRS1915+105 as a means to probe the production of relativistic plasma that

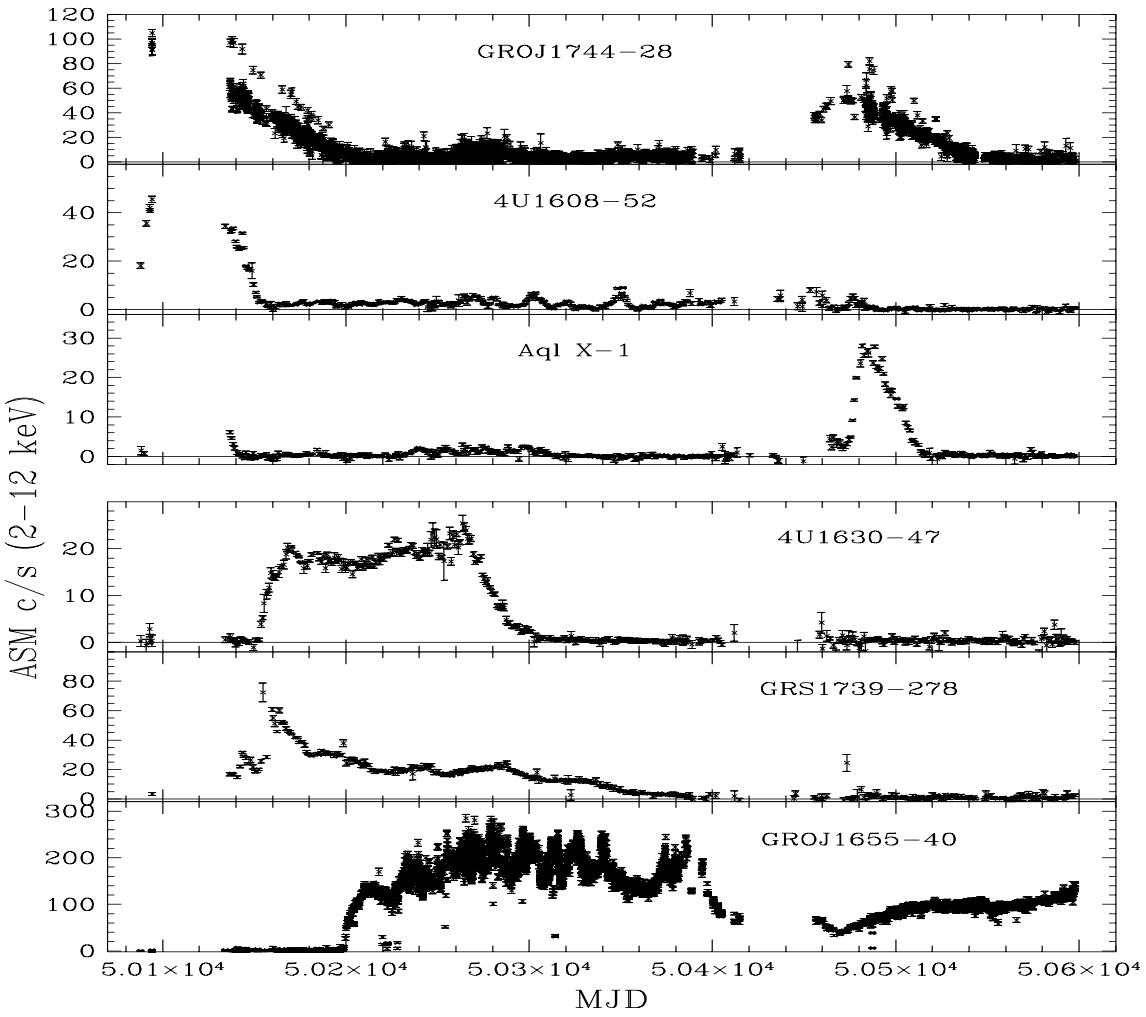

Fig. 1. ASM light curves for six bright X-ray transients over the time period 1996 Jan to 1997 May. The top three sources are accreting neutron stars, while the bottom three are black hole binaries or candidates. The Crab Nebula produces as ASM rate of 75.5 c/s.

powers the radio flares and jets in this system.

Turning to other transient X-ray sources, most of the two outburst cycles in GROJ1744-28 were covered with RXTE, as was the prolonged outburst in a new transient, GRS1739-278. Major eruptions were also seen in the recurrent transients 4U1608-52, Aql X-1, and 4U1630-47. The ASM light curves for these 6 sources are shown in Figure 1. Rapid rise with a brief maximum and an extended period of low-level emission characterizes both neutron star systems Aql X-1 and 4U1608-52. In contrast, 4U1630-47 rises quickly but then reaches its luminosity peak very slowly, with an increasingly hard spectrum, before it decays rapidly (e-fold time of 14 days) with no further signs of brightness enhancment. In the case of GRS1739-278, complex secondary brightening events are seen and the spectrum becomes increasingly soft with time. All of these ASM results complement earlier investigations from more limited X-ray monitoring missions (see Chen, Shrader, and Livio 1997). The shapes and spectral details of these outbursts provide substantial challenges for the disk instability models being applied to soft X-ray transients (e.g. Cannizzo, Chen, and Livio 1995; Narayan, McClintock, and Yi 1996). Particular support for this model was gained with the detection of an optical precursor to the April 1996 X-ray ouburst in GROJ1655-40 (Orosz et al. 1997). The 6-day delay time in the X-ray rise, relative to optical brightening, has been interpreted in favor of advection-dominated accretion during the brief period of X-ray quiescence prior to this event (Hameury et al. 1997).

ASM light curves are also available for a number of fainter X-ray transients, as shown in Figure 2. These results are displayed in 1-day or 2-day time bins. Of these 6 cases, only the Rapid Burster and RXJ1709-266 were known prior to 1996. Again, there is a broad diversity in the time scales for both X-ray decay and recurrence. Fur-

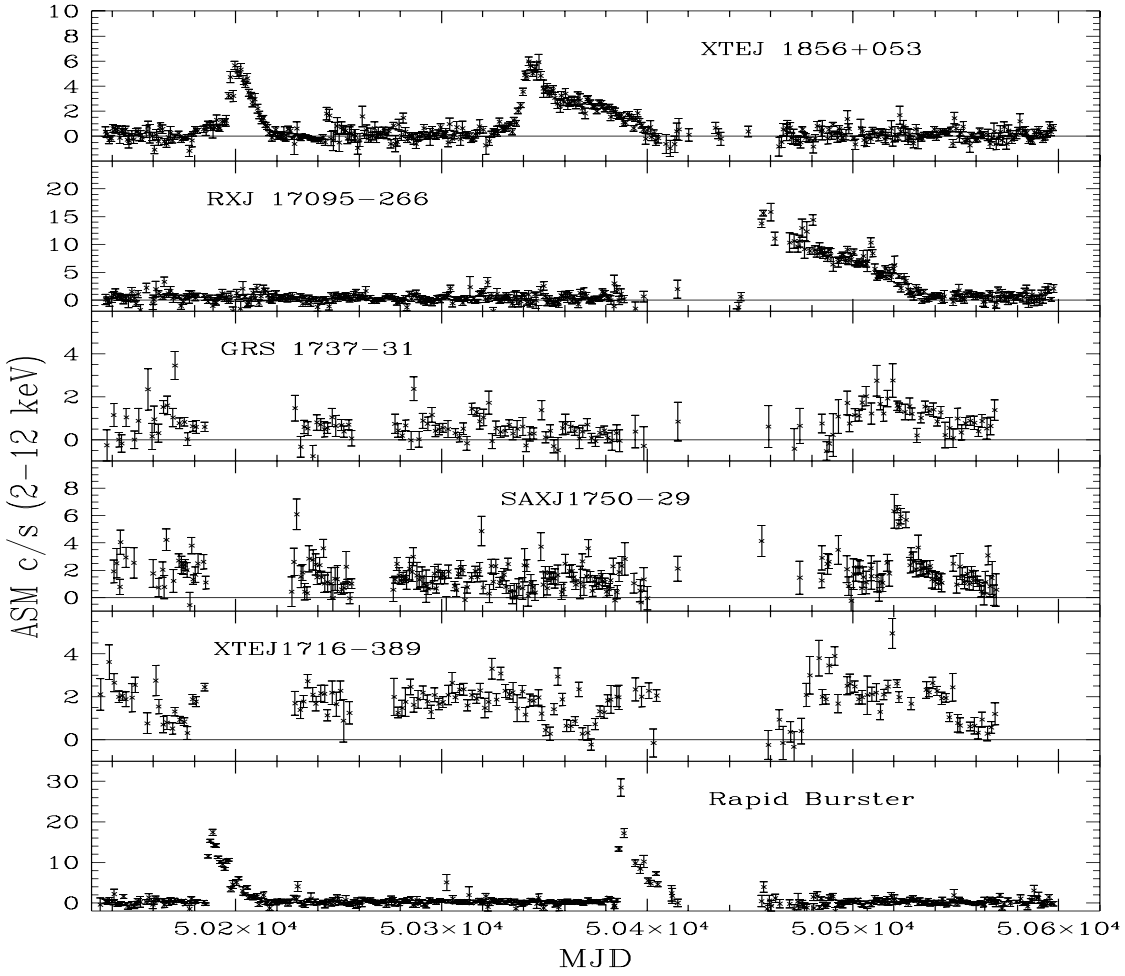

Fig. 2. ASM light curves (1996 Feb to 1997 May) for six faint X-ray transients. Only the Rapid Burster and RXJ17095-266 were known prior to 1996.

ther examples are needed in order to determine whether the fainter X-ray transients can be understood as more distant examples of the same parent populations that produce the bright transients.

3.2. Binary Periods and Super-Orbital Periods

The ASM has already accumulated about two dozen detections of orbital or "superorbital" periods, ranging from the well-known eclipsing neutron star systems with massive supergiant companions to the more subtle and less regular periodicities frequently associated with geometric effects related to the precession of an accretion disk inclined with respect to the binary plane. The paper by Corbet in this conference proceedings is devoted to the theme of orbital and super-orbital periods detected with the RXTE ASM, and readers are referred to that work for further information on this topic.

3.3. State Changes in X-ray Binaries

The topic of aperiodic variability in X-ray binary systems is very rich and complex, and a thorough description of the applications for ASM data is well beyond the scope of this paper. However, one aspect of this phenomenology, that of state changes in X-ray binaries such as Cyg X-1, Cyg X-3, and the "microquasars", may serve to illustrate the productivity to be gained by coordinating the observations of wide-field monitors with those of larger, pointing instruments.

Both GRS1915+105 and GROJ1655-40 migrate through different X-ray emission states (e.g. MGR97) on time scales of 3-20 weeks, as evidenced by correlated changes in the characteristics of the ASM light curves, the photon spectrum, the shape of the PCA power spectrum, and the properties of X-ray quasi-periodic oscillations (QPO). The cause of these transitions remains one of the fundamental mysteries associated with black

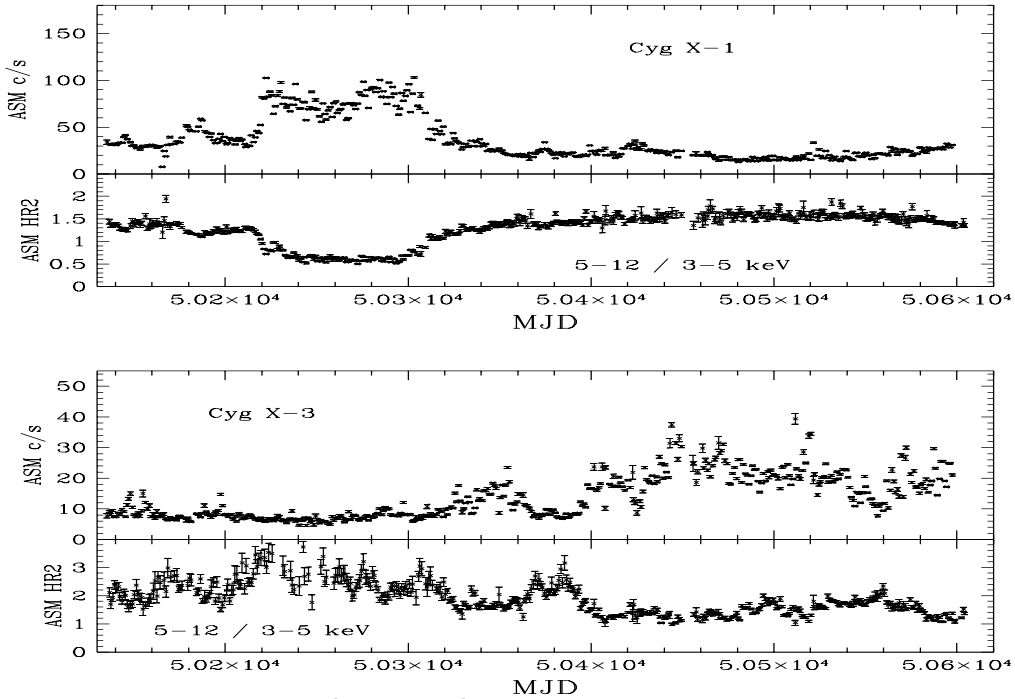

Fig. 3. ASM light curves and hardness ratios for Cyg X-1 and Cyg X-3 over the time period 1996 Feb to 1997 May. HR2 is the ratio of the flux in the 5-12 keV band to that in the 3-5 keV band.

hole accretion, the evolution of X-ray novae, and the mechanism of QPOs. A particularly important aspect of this science concerns the stationary, high-frequency QPOs seen at 67 Hz in GRS1915+105 (MGR97) and at 300 Hz in GROJ1655-40 (Remillard et al. 1997). The origin of these QPOs is likley founded in general relativity, with the QPO frequency dependent on the mass and rotation of the black hole. While it is not yet clear how to interpret these high-frequency QPOs, there is strong evidence that their appearance is correlated with X-ray emission states. The ASM light curves are particularly valuable in providing context for these investigations and in planning future RXTE observations when the X-ray state implies that these QPOs are likely to recur.

The ASM has also captured the more classical state transitions to the "soft X-ray high state" in both Cyg X-1 and Cyg X-3. Figure 3 shows the ASM light curve and spectral hardness ratio for these sources. In each case, a 30-day interval with moderate spectral softening preceeds the main event. In the case of Cyg X-1, the combined coverage of RXTE and BATSE has demonstrated that there is only a slight (15%) increase in total luminosity during the soft/high state (Zhang et al. 1997). Detailed temporal and spectral analyses of RXTE observations further indicate that the inner edge of the accretion disk is significantly closer to the black hole event horizon in the soft/high state, while the power-law component (associated with inverse Compton emission from energetic electrons) switches from a flatter spectrum with a thermal cutoff, in the low/hard state, to a steeper spectrum without a thermal cutoff from a small emission cloud in the soft/high state (Cui et al. 1997). The full ramifications of these geometric changes are still under investigation.

In the case of Cyg X-3, the soft/high transition has also led to the formation of a radio jet with a velocity that may be as high as 0.9 c (Ghigo et al. 1997). This high-state episode is still in progress, and the full story is yet to be told. Again, the monitoring efforts from the ASM, BATSE, and the GBI telescope are vital elements to be combined with observations from the VLA and RXTE pointing instruments in the effort to understand what has happened to Cyg X-3 during 1997 and what conditions led to the succession of the radio events that are still underway.

3.4. Active Galactic Nuclei

With a 30 mCrab detection threshold per SSC-dwell, it was not expected that the RXTE ASM would have the sensitivity necessary to provide useful information on the different subclasses of active galactic nuclei (AGN). There are only a few AGN expected to exceed 3 mCrab at 2-12 keV (e.g. Wood et al. 1984). However, the ability to combine the individual ASM measurements into 1-day or 2-day time bins without encountering significant fluctuations from systematic problems allows the ASM to monitor many nearby AGN for major changes in X-ray brightness. Six examples are shown in Figure

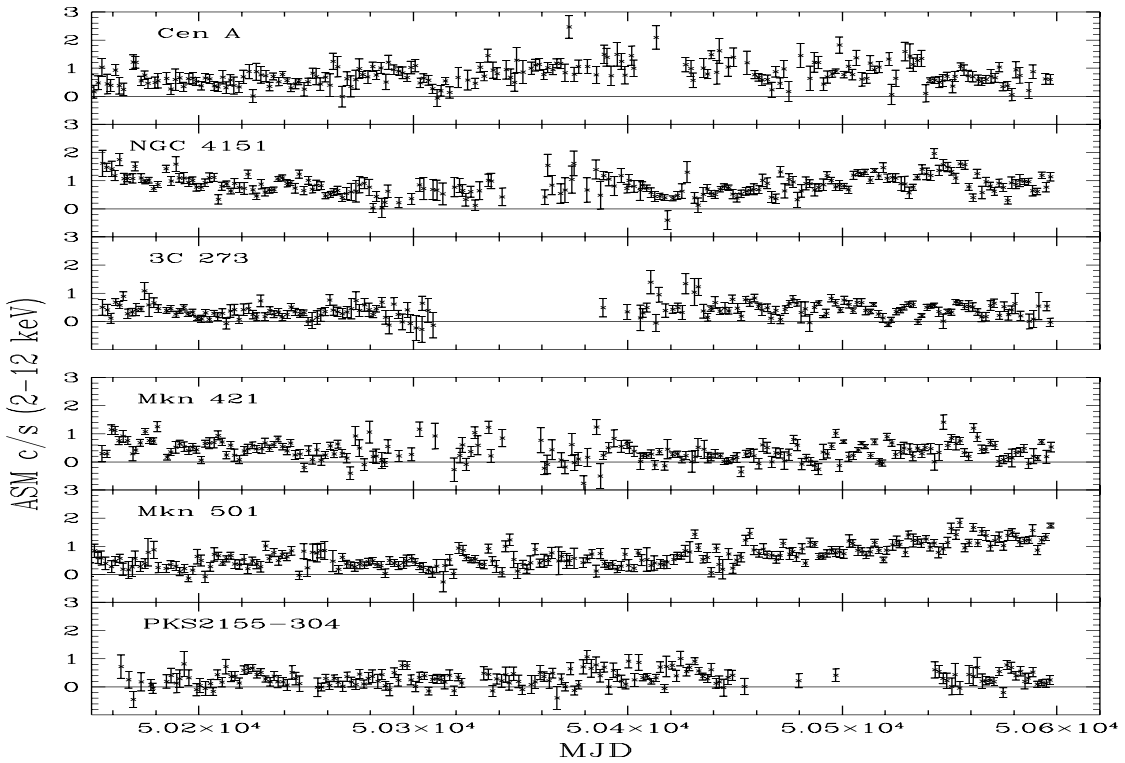

Fig. 4. ASM light curves of Cen A, an optically obscured AGN, the Seyfert 1.5 galaxy NGC 4151, the quasar 3C273, and 3 BL Lac objects. The data are displayed in 1-day or 2-day bins.

4. Both Cen A and NGC 4151 vary by a factor of two, and the flux from NGC 4151 reaches 24 mCrab at 2-12 keV. A major outburst in the BL Lac object Mkn 501 began during 1997 January (near MJD 50450), with X-ray intensity rising from 3 to 20 mCrab. This outburst is correlated with strong detections of Mkn 501 in TeV γ-rays with the HEGRA Cherenkov array (Aharonian et al. 1997). The TeV and X-ray components are very likley to be inverse-Compton and synchrotron photons emitted by the same parent population of relativistic electrons. These exciting results and the opportunities for further detections of AGN outbursts has led us to increase the total number of ASM-monitored emission-line AGNs and BL Lac objects from 10 to 74 during 1997 May.

References

Aharonian, F. et al. 1997, A&A, submitted, astro-ph/9706019

Cannizzo, J. K., Chen, W., and Livio M. 1995, ApJ, 454, 880

Chen, W., Shrader, C. R., and Livio, M. 1997, ApJ, in press, astro-ph/9707138

Cui, W., Zhang, S. N., Focke, W., and Swank, J. H. 1997, ApJ, 484, 383

Ghigo, F. D. et al. 1997, Bull. AAS, 29, 841

Hameury, J. M., Lasota, J. P., McClintock, J. E., and Narayan, R. 1997, ApJ, submitted; astro-ph/9703095

Levine, A. M. et al. 1996 ApJL, 469, L33

Morgan E. H., Remillard, R. A. and Greiner, J. 1997, ApJ, 482, 993

Narayan, R., McClintock, J. E., and Yi, I. 1996, ApJ, 457 821

Orosz, J. A., Remillard, R. A., Bailyn, C., and McClintock, J. E. 1997, ApJL, 478, L83

Remillard, R. A. et al. 1997, Procs. Texas Symposium on Relativistic Astrophysics (1996 December), in press; astro-ph/9705064

Ritter, H, and Kolb, U. 1995, in X-ray Binaries, eds. Lewin and van Paradijs (Cambridge: Cambridge Univ. Press), 578

Wood et al. 1984, ApJS, 56, 507

Zhang, S. N. et al. 1997, ApJL, 477, L95